

CHAPTER 62

EXPERIMENTAL INVESTIGATION OF SHOCK PRESSURES AGAINST BREAKWATERS

Gustaf Richert

Tech.lic., Division of Hydraulics
Royal Institute of Technology, Stockholm
Sweden

ABSTRACT

This paper describes an experimental investigation of shock pressures against breakwaters caused by breaking waves. The study only considers shocks of a compressive type, which occur if the wave front is formed in such a way that an air cushion is entrapped between the wave and the wall. In this case the compression and expansion of the air cushion plays an important rôle in the pressure variation.

Only waves preceded by non-breaking waves were used. For different combinations of bottom geometry and water depth the occurrence of shock pressures of different magnitudes was studied varying the wave height and the wave period. For some interesting combinations of bottom geometry and wave dimensions a series of tests were made to investigate the distribution over the wall of shock pressure and of shock impulse. The results, presented in diagrams and tables, have been commented on and analysed with special respect to the chosen test procedure.

INTRODUCTION

The previous research presents a very scattered view on the shock pressure problem. Different bottom slopes from 1:50 (MITSUYASU) to 1:2 (NAGAI) have been tested. Different test procedures have also been used: Solitary waves (e.g. BAGNOLD, DENNY, HAYASHI-HATTORI) and consecutive breaking waves (e.g. RUNDGREN, MITSUYASU) have been studied. The pressures have been measured using different methods, and sometimes the equipment, often insufficiently described in the reports, have, in view of later investigations, been of a too low natural frequency. The results are often contradictory and have been presented in different ways. This regards the characterisation of the waves as well as of the pressure, its duration and distribution and the pressure impulse. Thus, it is extremely difficult to compare the results of different authors or to formulate distinct tendencies for the relations between the shock pressure characteristics, the wave characteristics and the boundary geometries.

For the designing engineers, there are still several deficiencies of knowledge. - In spite of the work by CARR (1954), very little is known about the occurrence of shock pressures. Which combinations of wave period and wave height are, for different combinations of bottom slope and water depth, expected to give shock and which are not. - Apart from a few tests by ROSS (1955) breaking

waves preceded by nonbreaking waves have not been systematically investigated. Since such waves are likely to occur in nature and since solitary waves usually give higher pressures than corresponding consecutive breaking waves, this type of wave - the breaking wave preceded by nonbreaking waves - should be of interest.

Not much is known about the probable and possible horizontal distribution of shock pressures. In spite of the systematic work of NAGAI (1960) more information is needed on the simultaneous vertical pressure distribution against a wall. Contradictory results have been published on this subject.

The main purpose of this investigation has been to fill in some of these deficiencies of knowledge.

TEST INSTALLATIONS

The tests were carried out in a flume which is 1.2 m wide, 0.8 m deep and which has a total length of 19 m, 13.5 m of which a horizontal bottom, see Fig. 1. A flap-type wave generator was hinged at the bottom of the deeper part

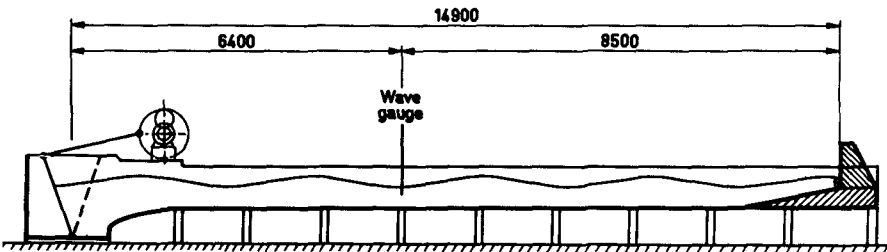


Fig. 1. Test Installations

of the flume. This wave generator can produce regular waves of different periods and amplitudes, the maximum period being about 1.67 s.

At the opposite end of the flume, 14.9 m from the wave generator, a plane test wall was placed on a built-in bottom. This wall consisted of a 15 mm thick steel plate, which was screwed onto a system of 10 vertical buttresses made of concrete and with flanges of steel. The test wall could oppose the waves with its front vertical or sloping 30° to the vertical. Two of the buttresses were designed in such a way that the pressure gauges could be installed between them. 100 x 100 x 15 mm mounting plates into which the pressure gauges were fitted, could be screwed onto the flanges of the buttresses with their surfaces flush with the front plate. The centerline of the vertical row of gauges situated 122 mm to the right of the center line of the flume. Since the pressure gauges could not be placed closer than with their centers 100 mm apart it was made possible to place the set of three gauges at different levels. Thus the vertical pressure distribution could be studied more in detail by repeating

the test runs for the different levels of the pressure gauge set. During the investigation the set of gauges was placed at levels with the center of the lowest gauge 2.2 cm, 4.0 cm, 5.7 cm and 9.0 cm above the bottom of the wall.

In a similar way it was made possible to investigate the horizontal pressure distribution on an arbitrary level. On this level pressure gauges could, besides the one placed 122 mm to the right of the centerline of the flume, be placed 143 mm and 388 mm or alternatively 266 mm and 511 mm to the left of the centerline of the flume.

The gauges were mounted so that the sensitive membranes were flush with the wall. The fissures around the gauge mountings were carefully tightened with plastic material in order to prevent compressed air or the entrapped air cushion to escape that way.

The buttresses, their flanges and the mounting plates for the gauges were calculated to have natural frequencies of at least 10^4 Hz. Any disturbances resulting from oscillations of the test wall or from shock waves reflected within the construction elements were not observed.

The built-in bottoms on which the test wall was placed were of different types. The ones with the slope 1:3 were designed to correspond to the rubble mound of an average composite-type breakwater. In the previous research regarding composite-type breakwaters (e.g. NAGAI, 1960), usually the horizontal width of the top of the mound in front of the wall, a , equals the water depth in front of the wall d_1 . Thus, to facilitate comparisons, the width was chosen a 15.0 cm, the same as the most used water depth. In order to get results for values of the ratio d_1/a larger than 1, tests were also made on a mound with a horizontal width a of 7.5 cm. In that way attempts could be made to reproduce the larger tests with a linear scale of 1:2. The mound with $a = 15.0$ cm had a height of 36.9 cm above the bottom of the flume while the one with $a = 7.5$ cm had a height of 39.1 cm.

Tests were also made with the wall standing on bottoms with slopes corresponding to natural ones and without horizontal planes on the top. It was first intended to use only the slope 1:10 but, since the results showed important differences to the results for the slope 1:3 tests were also made with bottom slopes of 1:6 and 1:25. The built-in bottoms with natural slopes had a height of 37.2 cm above the bottom of the flume, which is nearly the same as the heights of the rubble mound mentioned above.

RECORDING EQUIPMENT

Wave dimensions. - The heights and the periods of the waves were measured by a resistive water level gauge placed 8.5 m from the test wall. The resistance variations were recorded with the help of an ABEM coil galvanometer recorder which had a paper speed of 2.5 or 5.0 cm/s.

Behaviour of waves. - The action of the waves immediately in front of the wall could be photographed through the glass wall of the flume. The camera was a Paillard Bolex 16 mm Movie Camera, used with a speed of 64 pictures/s. 5 test runs were photographed for each combination of wave height, period and boundary geometry for which the pressure distribution was investigated. All other waves were watched through the glass wall of the flume and their behaviour was noted.

Wave pressures. - The pressure gauges used were of the capacitive type, specially designed for shock pressures by TBR, Delft. A gauge of this type consists of a membrane with 20 mm diameter, which forms one of the electrodes in a capacitor, see Fig. 2. A capacitive displacement meter which fed the gauges with a constant

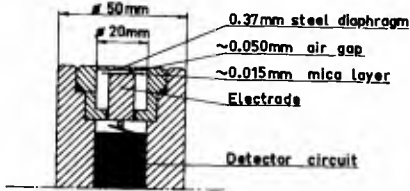


Fig. 2. Pressure gauge.

carrier frequency of 1050 kHz also translated the capacitance variations caused by membrane deflections into signals which were recorded by the galvanometer recorder and by an oscilloscope. Since the capacitive displacement meter had only three channels, pressures could be measured at only three points simultaneously. The natural frequency of the pressure gauges was 5500 Hz when they were submerged in water and 8800 Hz in air.

By means of coil galvanometers with a natural frequency of 8000 Hz, the pressure variations could be recorded on the same paper as the corresponding wave form. In spite of the fact that the paper moved very slowly and the sensitivity of the very fast galvanometers was low, this arrangement proved very useful. The wave which had caused the shock pressure recorded by the oscilloscope could be identified and the order of magnitude of the pressure registration could be checked.

An oscilloscope of a very suitable type, Tectronix 564, was used to study the pressure variations in detail. This oscilloscope is equipped with a storage system, which stores the trace of the sweep on the screen for some time. This made it possible to study the pressure variation and to decide whether it was worth photographing or not. The trace of the sweep could be photographed with a special oscilloscope polaroid camera, a typical photo of which is shown in Fig. 3.

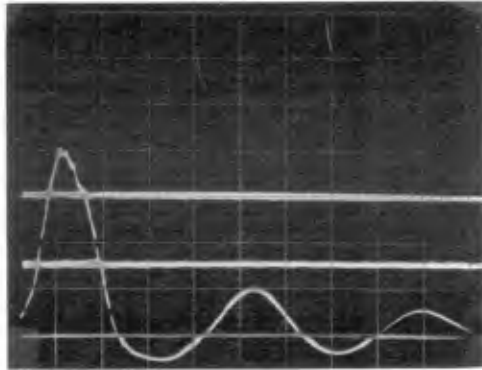


Fig. 3. Oscilloscope photo.

The oscilloscope sweep was started by a trigger mechanism when the pressure reached a certain height.

The pressure recording equipment was calibrated statically with compressed air pressures, after about 200 test runs or when the electrical conditions were changed significantly. The pressure of the air was measured with a mercury manometer. The calibration diagrams showed very small variations from one calibration to another.

TEST PROCEDURE

When a breaking wave hits a vertical wall spray is thrown upwards into the air and the water in front of the wall is mixed with air bubbles. The disturbances caused by the downfall of the spray and by bubbles from the preceding wave are not reproduced in a correct way in model tests. Furthermore, these disturbances would soften the shock pressure. Consequently it was found more interesting and necessary to study the shock pressures caused by breaking waves preceded by non-breaking waves. Such a combination is likely to occur in a prototype.

Thus, the following procedure for the tests was chosen. Before each test run, the wave generator was put in a certain position. The test run was not started until the water surface in the flume was calm. When the wave generator started the beginning of a wave train travelled towards the test wall. As a rule, the 4th wave of this wave train was studied, but occasionally, especially when the wave period was short, it proved necessary to study the 5th, the 6th or even the 9th wave. In a few cases, for the shoal with $a = 7.5$ cm, the 3rd wave was studied.

For each combination of bottom geometry, water depth and wave period different values of the wave generator amplitude were tested. This amplitude was decreased until the studied wave became so small that it could not break against the test wall but only produced clapotis. On the other side, the amplitude could not be increased too much owing to three reasons:

1. The studied wave became so high that it broke too far from the test wall to produce any shock pressure.
2. The wave preceding the studied wave broke or otherwise produced too much disturbance.
3. The top of the studied wave broke when passing the wave gauge.

In the case of 2 and 3 no upper limit for the occurrence of shock pressures could be determined.

For the 1:25 shoal some tests were carried out with a series of consecutive breaking waves.

TEST PROGRAM

The influence of wave height and wave period on the occurrence and magnitude of shock pressures was investigated using several combinations of bottom geometry and water depth. The combinations which have been studied are indicated in

Table 1. The geometry characteristics are defined in Fig. 4.

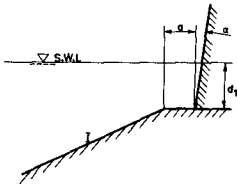


Fig. 4. Definitions of geometry characteristics.

During these investigations, the center of the lowest pressure gauge was normally situated 5.7 cm above the bottom of the wall. It was attempted to make model scale studies at a scale difference of 1:2 by studying tests with $a = 15.0$ cm, $d_1 = 15.0$ cm and $a = 7.5$ cm, $d_1 = 7.5$ cm respectively. Thus, in the tests with $a = 7.5$ cm the gauges were moved to more comparable positions, with the center of the lowest gauge 2.2 cm above the bottom of the wall.

I	a cm	α °	d_1 cm			
			5.0	7.5	11.0	15.0
1:3	15	0			x	x
1:3	7,5	0		x		x
1:6	0	0		x	x	x
1:10	0	0		x	x	x
1:25	0	0	x	x	x	x
1:3	15	30			x	x

Table 1. Investigations of occurrence of shock pressures.

Some dangerous or otherwise interesting combinations of wave period and wave height were selected, see Table 2. For each of these combinations 25 tests

Series	I	a cm	α °	d_1 cm	T s	H cm
A	1:3	15	0	15.0	1.40	19.40
B	1:3	15	0	15.0	1.40	20.30
C	1:3	15	0	15.0	1.64	13.30
D	1:3	15	0	11.0	1.30	16.60
E	1:3	7,5	0	15.0	1.50	20.50
F	1:10	0	0	11.0	1.50	11.80
G	1:3	15	30	15.0	1.40	19.90
H	1:3	15	30	15.0	1.40	21.00

Table 2. Investigations of pressure and impulse distributions.

with identical conditions were made for each position of the gauges and the pressure and impulse distributions were evaluated statistically. Since, in the tests with the nonvertical wall, the dispersion of the results was comparatively small, it was decided upon to make 10 runs only for each gauge position.

The extent of the test program was worked out continuously with regard to the results.

INTERPRETATION OF RESULTS.

Wave dimensions. - The wave form registered on the galvanometer recorder paper made it possible to measure wave heights and wave periods. The wave lengths were calculated with the formula

$$L = \frac{gT^2}{2\pi} \tanh \frac{2\pi d}{L} \quad (1)$$

Fig. 5 shows how the height (H) and period (T) of a particular wave were defined and measured on the registration.

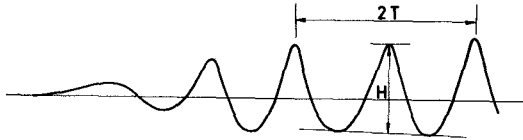


Fig. 5. Definitions of wave characteristics.

The wave dimensions at the point where the wave gauge was situated have been recalculated to dimensions valid for points of interest for a designing engineer. For the tests with bottom slopes of 1:6, 1:10 and 1:25 the wave heights given in this paper represent the dimensions of the studied wave when it passed over the point of the bottom where $d = 0.1L_0$. It is assumed that Stokes theory for finite amplitude waves is valid for $d \geq 0.1L_0$. ($L_0 = gT^2/2\pi = 1.56T^2$)

For the tests with the bottom slope 1:3, on the other hand, the waves are valid for the depth of water between the water surface and the bottom of the flume. Assuming this depth being constant in the flume, the recorded wave dimensions have been recalculated as described below to the section of the flume where, during the tests, the water depth was $d = 0.1L_0$ over the built-in sloping bottom. Thus, the wave dimensions given in the paper represent what the waves would have been in that section of the flume if the composite-type break-water construction had not existed.

A theory given by SVERDRUP-MUNK, 1947, was used for the recalculation of the wave dimensions. It assumes that the potential energy of a wave is transmitted with the wave velocity while the kinetical energy is stationary. The potential energy can be calculated from the formula

$$\frac{E_{\text{pot}}}{E_{\text{tot}}} = n = \frac{1}{2} \cdot \sqrt{1 + \frac{4\pi d}{L} \operatorname{sinh} \frac{4\pi d}{L}} \quad (2)$$

The distance (b) between the wave gauge and the point of interest as

described above was different for each combination of bottom geometry and wave period. For each combination the energy transport was calculated with significant mean values of water depth (d), wave length (L) and energy ratio (n). The total energy of the n th wave at the gauge and at the actual point of interest could be determined as the energy of the n th wave $n + 6.40/L$ periods and $n + (6.40 + b)/L$ periods after the start of the wave generator respectively. Thus, the ratio E/E_{gauge} between the total energy of an arbitrary wave at the point of interest and the total energy of the same wave at the wave gauge could be determined.

In the expression for the wave energy

$$E = \frac{\gamma}{8} LH^2 \cdot \left(1 - \frac{\pi^2 H^2}{2L^2 \cdot \tanh^2 \frac{2\pi d}{L}} \right) \quad (3)$$

the second term in the brackets is, for the waves in the test program, small compared to 1. Thus, Eq. (3) can, with good approximation, be simplified to

$$E = \text{const} \cdot L \cdot H^2 \quad (4)$$

A series of special tests were run in order to investigate the propagation of waves in the beginning of a wave train. These tests were made in a flume with constant depth and 20.5 cm width. The number of tests was 40 and the water depth and the wave dimensions were half of those used in the main tests. Wave gauges were installed at points corresponding to the wave gauge and to the test wall in the main tests. Behind the wave gauge corresponding to the test wall there was placed a wave absorber. The investigation showed that the wave period and hence the length of the studied wave corresponded at the two gauges with a maximum error of 4.2 o/o.

Thus Eq. (4) can be transformed into

$$\frac{H}{H_{\text{gauge}}} = \sqrt{\frac{E}{E_{\text{gauge}}}} \quad (5)$$

This expression was used for the calculation of the wave heights at the points of interest defined above.

The fact that the wave gauge was situated somewhat too near the wave generator affected the measured values of the wave dimensions in a manner which needs further comments. When the generated wave was very steep it lost its top and foam was created on the wave front before the wave passed the wave gauge. If the amplitude of the generator movement was decreased no such phenomenon occurred and the wave passed the wave gauge with unbroken top. Thus, although the generating energy in the second case was smaller, the recorded wave height could be somewhat larger due to differences in the wave form.

One example of this phenomenon was the relation between series A and B, see Table 2, for which the shock pressure distribution was investigated. In this case the generating energy of the studied wave was 8 o/o higher for the series A, while the measured wave height was 4 o/o higher for the series B. On the other hand the potential energy at the gauge was 2 o/o higher for the series A. Further-

more, the waves in series A behaved as if they were larger immediately in front of the breakwater. Hence, the wave height is not sufficient as characteristic of the wave in cases when the wave steepness is large. Anyhow, since the error was relatively small and since alternative wave characteristics are much more complicated to evaluate from large series of recordings, the wave height has, together with the wave period, been used as main characteristic of the wave form.

Occurrence of shock pressures. - The occurrence and magnitude of the shock pressures registered during this investigation are presented in Figs. 6 to 14. It must be observed that, as mentioned above, the pressure gauges during the studies regarding the occurrence of shock pressures were kept in a constant position. Thus, the pressure magnitudes do not represent maximum pressure peaks. (Compare the distribution diagrams.)

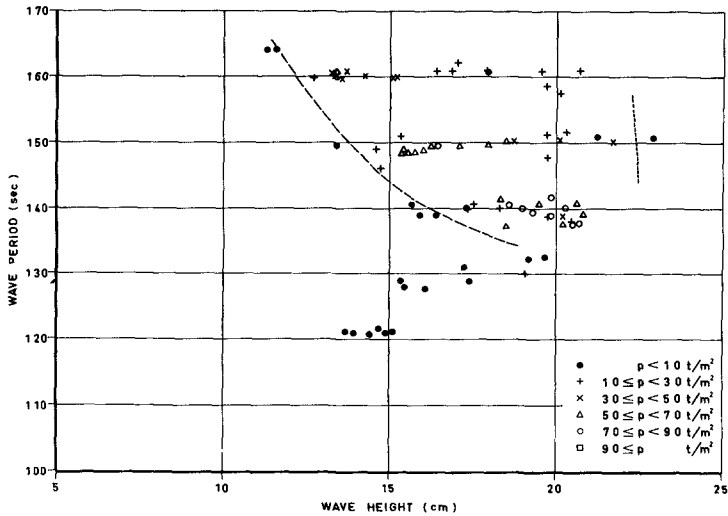


Fig. 6. Shock occurrence diagram. ($I=1:3$, $a=15$ cm, $d_1=15$ cm)

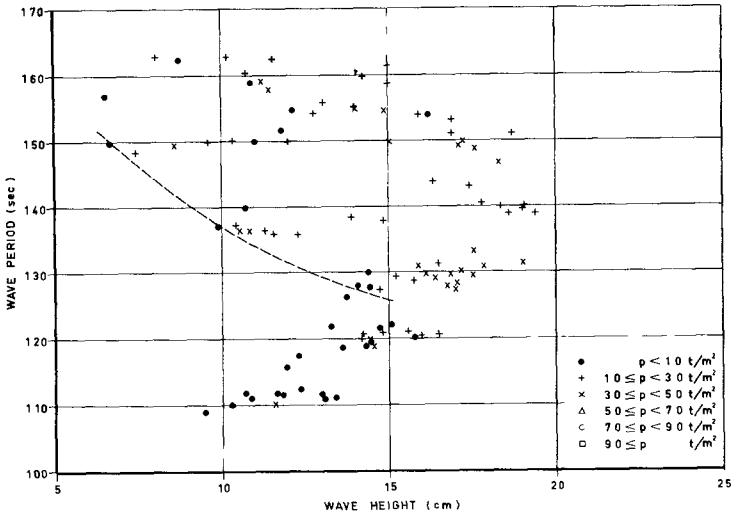


Fig. 7. Shock occurrence diagram. ($I=1:3$, $a=15$ cm, $d_1=11$ cm)

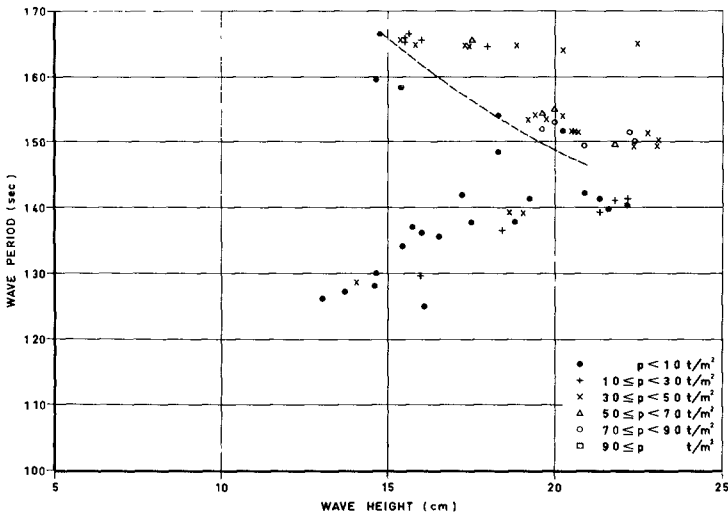


Fig. 8. Shock occurrence diagram. ($I=1:3$, $a=7.5$ cm, $d_1=15$ cm)

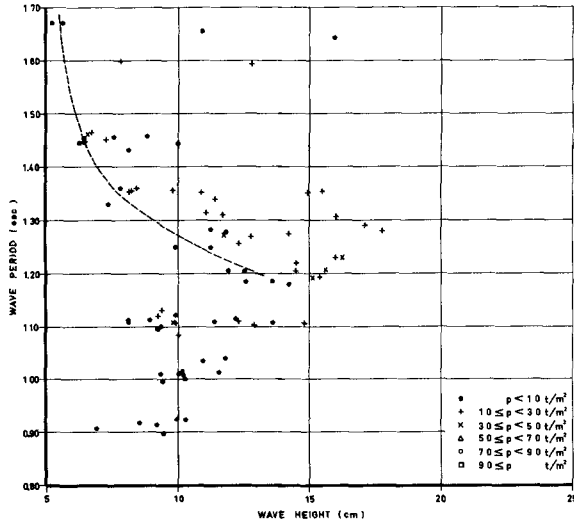


Fig. 9. Shock occurrence diagram. ($I=1:3$, $a=7.5$ cm, $d_1=7.5$ cm)

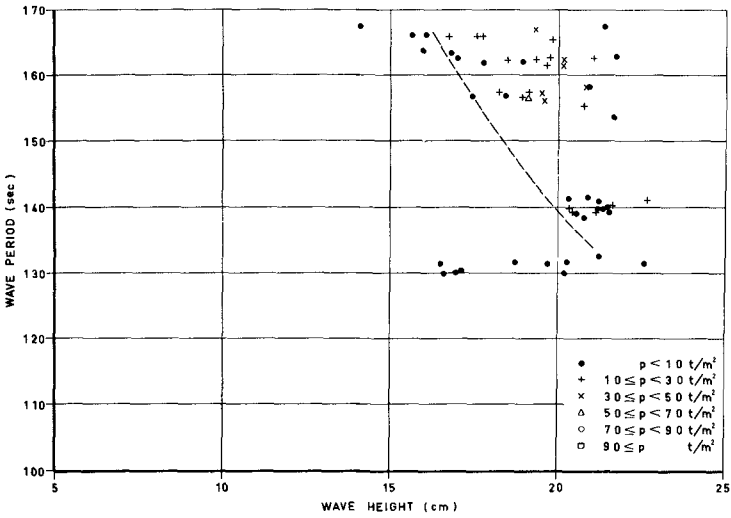


Fig. 10. Shock occurrence diagram ($I=1:6$, $d_1=15$ cm)

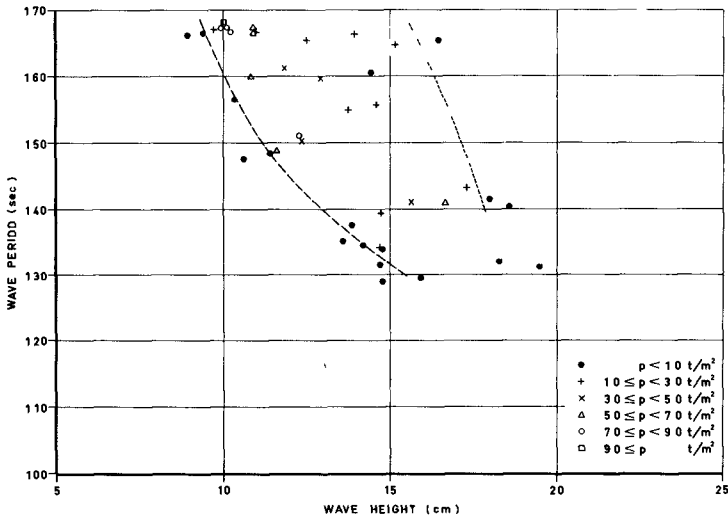


Fig. 11. Shock occurrence diagram. ($I=1:6$, $d_1=11$ cm)

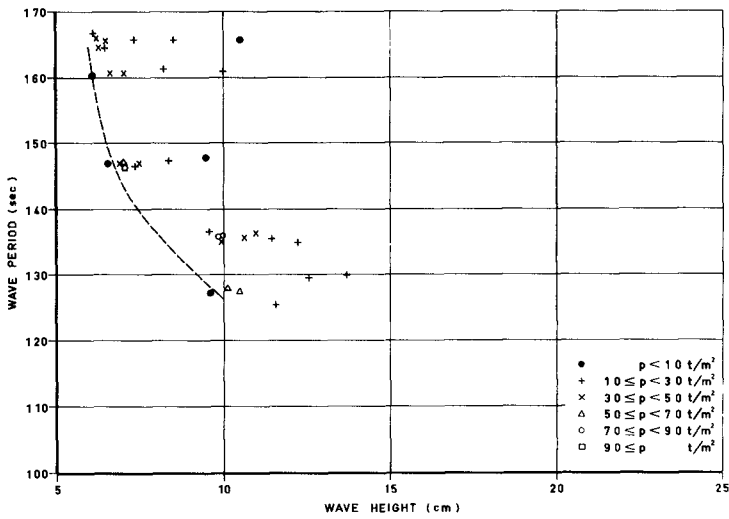


Fig. 12. Shock occurrence diagram. ($I=1:6$, $d_1=7.5$ cm)

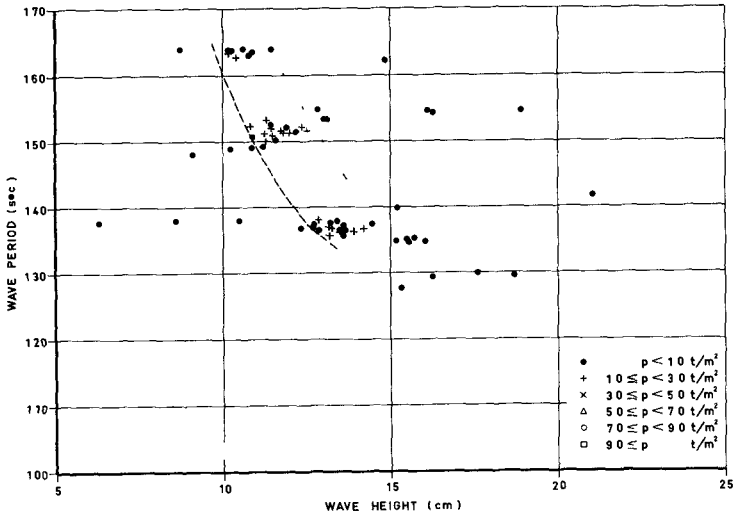


Fig. 13. Shock occurrence diagram. ($I=1:10, d_1=11$ cm)

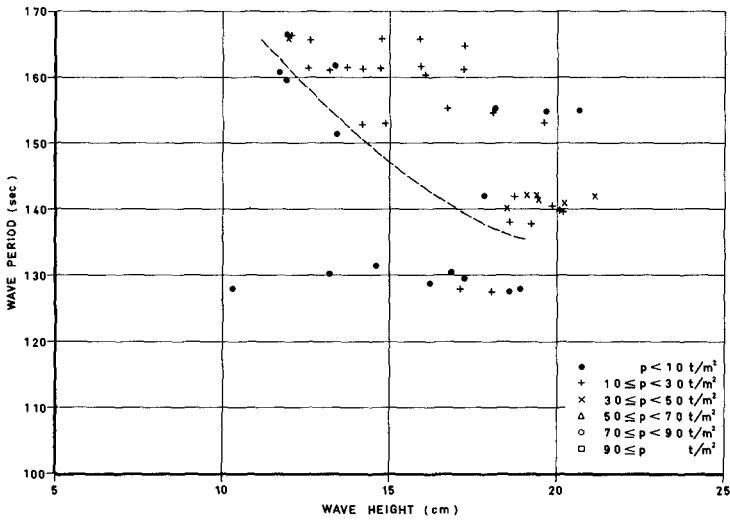


Fig. 14. Shock occurrence diagram. ($I=1:3, a=15$ cm, $\alpha=30^\circ, d_1=15$ cm)

The occurrence and magnitude of the shock pressures were directly dependent on the behaviour of the waves immediately in front of the wall. For a certain period, small waves did not break at all but only produced clapotis in front of the wall. These waves caused pressures against the wall, which were not large enough to start the oscilloscope sweep. Increasing the wave height, a certain, rather distinct value was reached, at which a thin air cushion was entrapped between the wave and the wall. A more distinct and sharp shock was heard and a short but very high shock pressure was recorded. After the first pressure peak the pressure decreased to below zero and then increased again continuing in a quickly damped oscillation. This oscillation can be explained as an adiabatic compression and expansion of the entrapped air cushion. The shortest recorded oscillation period was about 1.5 msec while the rise-time of the first peak corresponded to a somewhat shorter period. This rise-time was, however, very difficult to measure adequately since the time scale was limited by the capacity of the oscilloscope.

A further increase in wave height made the wave break in such a way that the air cushion grew thicker and hence the pressure became smaller but lasted for a longer time causing a longer oscillation period. Finally the wave became so high that it collapsed before it reached the wall. In these cases only very low shock pressures could be recorded if the oscilloscope sweep started at all. The upper limit of the occurrence of shock pressures was not so distinct as the lower limit.

The conditions described above could be observed for long wave periods. For short periods the waves needed a larger wave height to produce shock. However, for reasons given above, it was not possible to produce waves which had a large steepness at the test wall. Thus, it was usually impossible to establish the upper occurrence limit for shorter periods.

The behaviour of the waves in front of the breakwater was particularly affected by reflection phenomena in the test with the steepest bottoms and with short periods. Occasionally, waves which were too small to cause shock pressure against the wall met reflected preceding waves in such a way that parts of the wave were thrown against the wall. In that way shock pressures, although usually not very large, could be created by waves with short periods and lower wave heights than the normal lower shock occurrence limit. Such shock pressures have been recorded for all the tested relative water depths over shoals having a slope of 1:3, see Figs. 6 to 9 and 14.

As seen in Table 1, bottoms having slopes of 1:3, 1:6, 1:10 and 1:25 were tested. A comparison between the results confirms the observation by CARR (1954) that for a fixed wave period the range of wave heights creating shocks is narrower the flatter the slope of the bottom. It was also observed that, with the chosen test procedure, it was impossible to create violent shocks on the flatter slopes. The greatest shock pressure recorded at the shoal slope of 1:10 was 4.4 t/m^2 . Using the actual test procedure, no shock at all was recorded for the slope 1:25. However, some shocks, though rather weak, were recorded during tests having many consecutive waves in a wave train.

It was attempted to carry out different tests which were model tests to each other. Tests having a slope of 1:6 and depths of $d_1 = 7.5 \text{ cm}$, 11.0 cm and 15.0 cm could be considered to be corresponding scale models. At a slope of 1:3 only tests having a $a = d_1 = 7.5 \text{ cm}$ and a $a = d_1 = 15.0 \text{ cm}$ were scale models to each other.

If the occurrence diagrams of the test series which were corresponding scale

models were put in a dimensionless form they would coincide. For this purpose the wave heights have been recalculated to points with the depth $d = 3 d_1$. The adapted lower occurrence limit curves of the interesting tests have been represented in Fig. 15. The agreement between the curves is not perfect. This seems to be

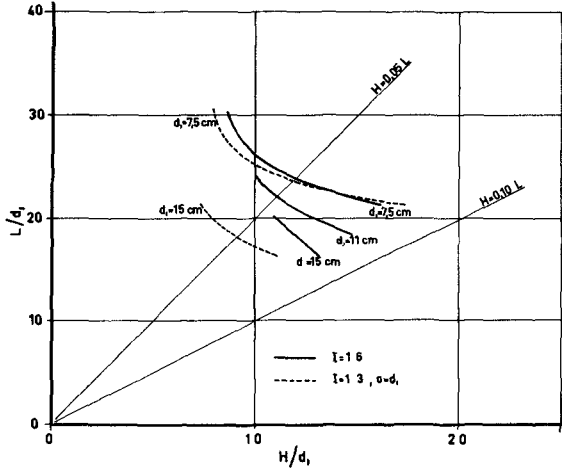


Fig. 15. Lower shock occurrence limits.

mainly due to the fact that even though the wave height H of the waves causing the shock pressures is in scale the preceding wave is not necessarily in the same scale. At smaller periods, the 5th, 6th, or even the 9th wave of the wave trains were studied. In these cases, the preceding waves were only slightly smaller than the studied ones, while on the other hand, the usually studied 4th wave was preceded by a considerably smaller 3rd wave. For shorter periods the studied wave was usually so disturbed by the preceding wave that it, in a sort of clapotis movement, lost parts of its top and hence lost energy before it reached the wall. Thus, for shorter periods, wave breaks and shock pressures were received only from waves having larger relative wave heights. Obviously, the simple notations of the period and height of one studied wave do not give a complete information about the behaviour of this wave. The mechanism of the breaking of a wave strongly depends on both the form of the actual wave and the behaviour of the preceding wave. This must be taken into account both in the planning of model tests for particular projects and in the interpretation of the results.

The influence of the horizontal width a of the top of the mound with slope 1:3 was easily noted by comparison between tests having $d_1 = 15.0 \text{ cm}$ and $a = 7.5 \text{ cm}$, see Fig. 7. Apparently, much larger waves were needed to produce shock pressures when the width a of the mound was small. The practical use of this information is so important that it should be specially observed.

A comparison between the tests with a vertical test wall and those with a

wall sloping 30° to the vertical gave two interesting results. First, it could be noted that at a water depth of $d_1 = 15.0$ cm curves representing the lower occurrence limit were almost identical. Secondly, it was not possible to create very large shock pressures against the sloping wall. Tests with a water depth of $d_1 = 11.0$ cm gave such small pressures and so insecure recordings that a shock occurrence diagram would have no meaning. These results seem to be logical as a breaking wave is not likely to have a water front with a hang-over sloping 30° without losing its top or otherwise showing the irregularities of the required late stage of breaking. Thus, no thin air cushion can be entrapped.

Pressure distribution. - The pressure distribution over the test wall was studied in 8 different cases, see Table 2. The results are represented in Figs. 15 to 23 where, for the different pressure gauge levels, the maximum, average and minimum values of the recorded pressures have been connected to form pressure distribution curves.

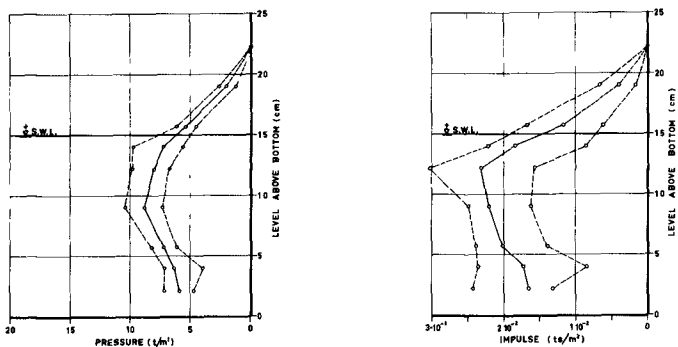


Fig. 16. Distribution diagrams. ($I=1:3$, $a=15$ cm, $d_1=15.0$ cm, $T=1.40$ s, $H=19.4$ cm)

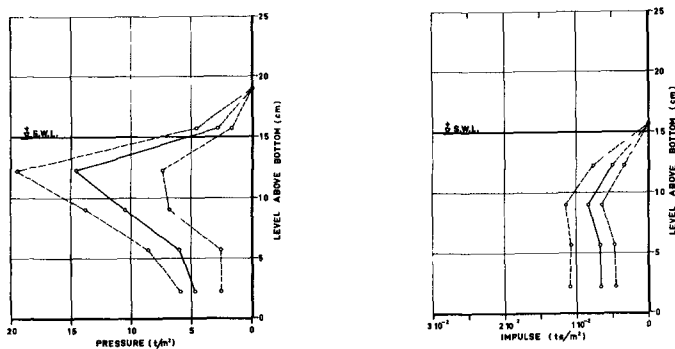


Fig. 17. Distribution diagrams. ($I=1:3$, $a=15$ cm, $d_1=15.0$ cm, $T=1.40$ s, $H=20.3$ cm)

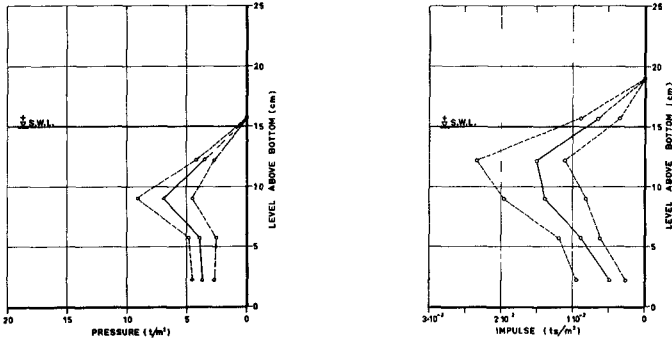


Fig. 18. Distribution diagrams. ($I=1:3$, $a=15$ cm, $d_1=15.0$ cm, $T=1.64$ s, $H=13.3$ cm)

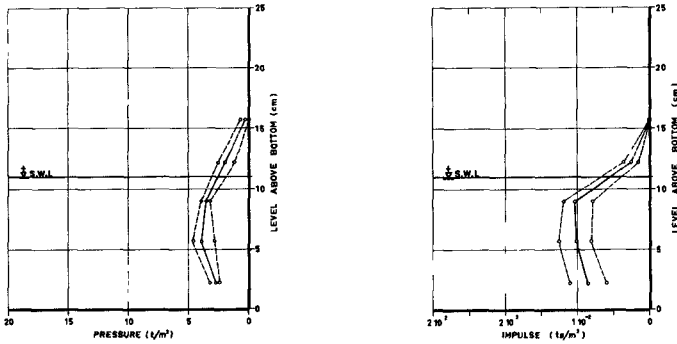


Fig. 19. Distribution diagram. ($I=1:3$, $a=15$ cm, $d_1=11.0$ cm, $T=1.30$ s, $H=16.6$ cm)

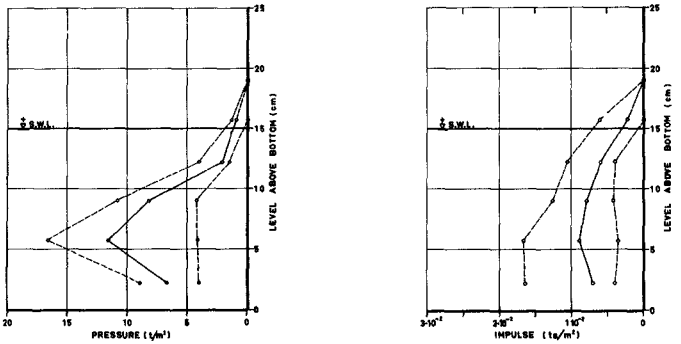


Fig. 20. Distribution diagram. ($I=1:3$, $a=7.5$ cm, $d_1=15.0$ cm, $T=1.50$ s, $H=20.5$ cm)

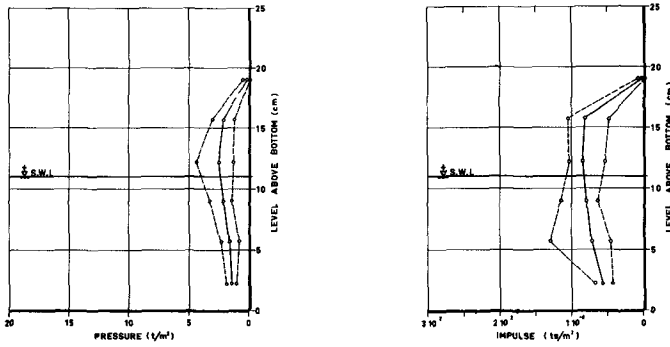


Fig. 21. Distribution diagram. ($I=1:10$, $d_1=11.0$ cm, $T=1.50$ s, $H=11.8$ cm)

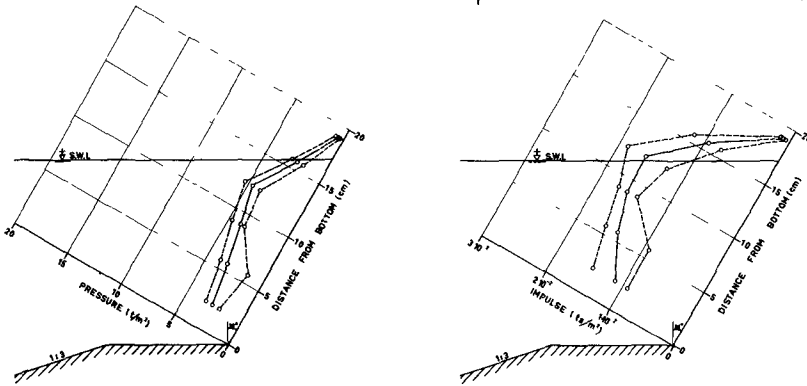


Fig. 22. Distribution diagram. ($I=1:3$, $a=15.0$ cm, $\alpha=30^\circ$, $d=15.0$ cm, $T=1.40$ s, $H=19.9$ cm)

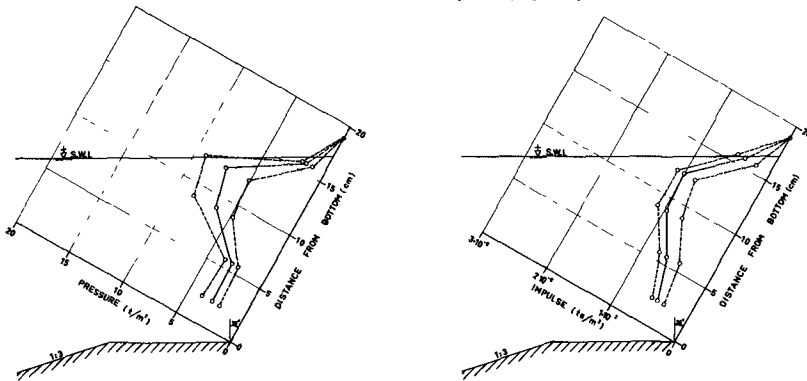


Fig. 23. Distribution diagram. ($I=1:3$, $a=15.0$ cm, $\alpha=30^\circ$, $d_1=15.0$ cm, $T=1.40$ s, $H=21.0$ cm)

A series of 25 tests was run (in the series with the sloping wall only 10 tests) for every level of pressure gauge recording the waves as well as the pressures. The wave height did not in any series deviate more than 7.5 o/o from the mean value. The corresponding maximum deviation for the wave period is only 1.8 o/o. The wave dimensions given in Table 2 are averages of the mean values for the different series. The mean wave height of the series never deviated more than 2.6 o/o from the average mean value given in the Table. The deviation of the mean wave period is quite negligible. These relatively low figures should be compared with the dispersion of the shock pressure magnitude as seen in the diagrams. Since, within each series, no correlation between the wave dimensions and the shock pressure could be discovered, this dispersion seems to be mainly due to occasional small disturbances of the wave front in the different tests. Such disturbances were impossible to detect since the movie films only showed the wave action just at the glass wall and not in the plane where the pressure gauges were placed.

Beside each pressure distribution diagram the corresponding impulse distribution diagram has been represented. The impulse (the surface under the pressure-time curve) has been calculated with a reasonable correction accounting for the first low part of the curve which has not been traced by the oscilloscope sweep. Since the period of oscillation was approximately the same at different levels, the pressure and impulse distributions are fairly congruent.

The maximum pressures occur simultaneously below a level corresponding to roughly 1.25 times the height above the bottom of the point where the convex part of the wave front first hit the wall. The higher regions of the average distribution curves where the shock pressure occurred later than below have been dashed. The comparison between the films and the distribution diagrams also gives the information that the largest pressure always occurred where the entrapped air cushion was initially situated.

A study of the different distribution diagrams can give extensive information on different aspects of the shock pressure phenomenon but in the following only some interesting features will be pointed out.

The largest pressures occur much lower in the tests with the bottom slope 1:3 than in those with the slope 1:10. This tendency is clearly confirmed by the movie films, which also indicate that the pressure distributions for the bottom slope 1:6 will be rather like the ones derived for 1:10. Thus, the resultant force was situated at 40-65 o/o of the still water depth above the bottom for the slope 1:3, while it was at 90 o/o above the bottom for the slope 1:10.

This observation, as well as the fact that the shock pressure against the test wall in no case decreased to zero at the bottom, differs from what has mostly been stated by other authors. This can be explained by the difference in test procedure and hence in the way in which the wave broke against the structures.

The movie films show that in the series A, the air cushion was not only thicker but also larger in the vertical direction than it was in the series B. This corresponds well to the general view of the pressure distribution which shows that in the series B there were higher but more local shock pressures. Thus, the resultant force was nearly the same in the two series while, on the other hand, the shock impulse in the series B was approximately half of the impulse in the series A. This is also in contrast to the statement by e.g. DENNY (1951) that a constant fraction of the forward wave momentum is transferred into shock impulse.

The tests regarding the horizontal distribution of the shock pressures gave

no special tendency. Sometimes the peak pressures occurred simultaneously over the whole width of the flume and sometimes not.

CONCLUSION

The present investigation gives results from tests with breaking waves preceded by non-breaking waves. These waves caused pressures which could be relatively high ($p_{\max} \approx 20 \text{ t/m}^2$ for a wave with $H \approx 20 \text{ cm}$) and also could have a short duration ($\approx 1 \text{ msec}$). The maximum pressures always occurred below the still water surface level and the shock pressures never decreased to zero at the bottom. This paper also presents shock occurrence diagrams which show the conditions for pressures of certain magnitudes to occur when different bottom geometries are used.

The present investigation only gives results for waves preceded by considerably lower waves. Such waves can cause comparatively high shock pressures for which the adiabatic compression of an entrapped air cushion plays a predominant role. This must be kept in mind when such tests are planned and when the results are converted to prototype scale.

ACKNOWLEDGEMENTS

The present investigation was carried out in the Laboratory of the Division of Hydraulics at the Royal Institute of Technology, Stockholm, Sweden. The author wishes to express his gratitude to Professor E. Reinius, Head of the Division, for his eminent leadership. The author also thanks the Swedish Board for Technical Development for supporting the investigation.

REFERENCES

- BAGNOLD, R.A. Interim Report on Wave Pressure Research. J. of the Inst. of Civ.Eng., June 1939.
- CARR, J.H. Breaking Wave Forces on Plane Barriers. Calif. Inst. of Tech., Hydr. Struct. Div., Rep. E-11.3., Nov. 1954.
- DENNY, D.F. Further Experiments on Wave Pressures. J. of the Inst. of Civ.Eng., June 1951.
- HAYASHI, T. and HATTORI, M. Pressure of the Breaker against a Vertical Wall. Coastal Eng. in Japan, 1958.
- MITSUYUASU, H. Experimental Study on Wave Force against a Wall. Coastal Eng. in Japan, 1962.
- MITSUYASU, H. Shock Pressure of Breaking Waves (I). Coastal Eng. in Japan, 1966.
- NAGAI, S. Shock Pressure Exerted by Breaking Waves on Breakwaters. A.S.C.E., Vol. 86, No. WW2, June 1960.
- ROSS, C.W. Laboratory Study of Shock Pressures of Breaking Waves. Beach Erosion Board, Tech. Memo No. 59, 1955.
- RUNDGREN, L. Water Wave Forces. Royal Inst. of Tech., Div. of Hydraulics, Bull. No. 54, 1958.
- SVERDRUP H.U. and MUNK, W.H. Wind, Sea and Swell. U.S.Navy Department., Hydr.Off.Publ. No. 601, 1947.